



ELSEVIER

Contents lists available at SciVerse ScienceDirect

Comptes Rendus Chimie

www.sciencedirect.com



Full paper/Mémoire

Crystal structure and ionic conductivity of $\text{AgCr}_2(\text{PO}_4)(\text{P}_2\text{O}_7)$

Brahim Ayed

Laboratoire de matériaux et cristallographie, département de chimie, faculté des sciences, Monastir, Tunisia

ARTICLE INFO

Article history:

Received 12 December 2011

Accepted after revision 9 May 2012

Available online 19 June 2012

Keywords:

Crystal growth
IR spectroscopy
X-ray diffraction
Structure

ABSTRACT

Single crystals of a new phosphate $\text{AgCr}_2(\text{PO}_4)(\text{P}_2\text{O}_7)$ have been prepared by the flux method and its structural and the infrared spectrum have been investigated. This compound crystallizes in the monoclinic system with the space group $C2/c$ and the parameters are, $a = 11.493(3) \text{ \AA}$, $b = 8.486(3) \text{ \AA}$, $c = 8.791(2) \text{ \AA}$, $\beta = 114.56(2)^\circ$, $V = 779.8(3) \text{ \AA}^3$ and $Z = 4$. Its structure consists of CrO_6 octahedra sharing corners with P_2O_7 units to form undulating chains extending infinitely along the $[110]$ direction. These chains are connected by the phosphate tetrahedra giving rise to a 3D framework with six-sided tunnels parallel to the $[101]$ direction, where the Ag^+ ions are located. The infrared spectrum of this compound was interpreted on the basis of $\text{P}_2\text{O}_7^{4-}$ and PO_4^{3-} vibrations. The appearance of $\nu_3\text{P-O-P}$ in the spectrum suggests a bent P-O-P bridge for the $\text{P}_2\text{O}_7^{4-}$ ions in the compound, which is in agreement with the X-ray data. The electrical measurements allow us to obtain the activation energy of (1.36 eV) and the conductivity measurements suggest that the charge carriers through the structure are the silver cations.

© 2012 Académie des sciences. Published by Elsevier Masson SAS. All rights reserved.

1. Introduction

During the past three decades, a number of phosphates belonging to the $\text{A}_2\text{O-M}_2\text{O}_3\text{-P}_2\text{O}_5$ ($\text{A} = \text{monovalent}$ and $\text{M} = \text{Al, Ga, Cr, Fe}$) system were showed to exhibit fast A^+ ion transport properties: among them are the Nasicon-type monophosphates $\text{A}_3\text{Cr}_2(\text{PO})_4$ and $\text{A}_3\text{Fe}_2(\text{PO})_4$ [1–4] the monodiphosphata $\text{Na}_7(\text{MP}_2\text{O}_7)_4\text{PO}_4$ [5] and the $\text{Na}_7\text{M}_3(\text{P}_2\text{O}_7)_4$ [6,7]. All these compounds have a 3D framework made up of corner sharing MO_6 octahedra and PO_4 tetrahedra, with the A^+ ions located in the interstitial space. During an attempt to find new materials with optimal properties and enrich this family of compounds, we successfully synthesized the solid-state compound $\text{AgCr}_2(\text{PO}_4)(\text{P}_2\text{O}_7)$.

This study reports its synthesis by the high temperature solid-state reactions and the single crystal structural determination are reported for the title compound, and the electrical conductivity has been measured as a function

of temperature. Furthermore, the infrared spectrum of $\text{AgCr}_2(\text{PO}_4)(\text{P}_2\text{O}_7)$ is reported and band assignments are made.

2. Experimental

2.1. Materials and measurements

All reagents were purchased commercially and used without further purification. A qualitative energy dispersive spectroscopy (EDX) analysis, performed on JEOL-JSM 5400 scanning electron microscope, revealed the presence of only Ag, Cr, P and O elements. The infrared spectrum for $\text{AgCr}_2(\text{PO}_4)(\text{P}_2\text{O}_7)$ was recorded at room temperature using single crystals on a Nicolet 470 FTIR spectrophotometer (resolution: 0.125 cm^{-1}), over the range $1400\text{--}400 \text{ cm}^{-1}$ using the KBr disk method. The impedance measurements were carried out in a Hewlett-Packard 4192-A automatic bridge monitored by a HP microcomputer. The frequency range was 5 Hz–13 MHz. Pellets of 13 mm diameter and 0.6 mm thickness were prepared by pressing the powder sample at 10 tones. Then the pellets were sintered at $600 \text{ }^\circ\text{C}$

Email address: brahimayed@yahoo.fr.

for 24 h. Silver electrodes were painted on the two faces of the pellets with a silver paste, and then the painted pellets were heated at 300 °C/h. The impedance measurements were carried out at steady-state temperatures on the pellets in still air.

2.2. Synthesis

Single crystals of $\text{AgCr}_2(\text{PO}_4)(\text{P}_2\text{O}_7)$ were prepared by crystallization in a flux of molybdate MoO_3 (Acros, 99%), in an atomic ratio P: Mo = 4: 1. Appropriate amounts of AgNO_3 (Fluka, 99%), $\text{Cr}(\text{NO}_3)_3 \cdot 9\text{H}_2\text{O}$ (Fisher, 98.6%) and $(\text{NH}_4)_2\text{HPO}_4$ (Merck, 99%) were mixed by dissolving in aqueous nitric acid and the obtained solution was dried at 353 K. The resulting dry residue was ground in an agate mortar to ensure its best homogeneity, and then gradually heated up to 873 K in a platinum crucible. After being reground, the mixture was melted for 1 h at 1123 K and subsequently cooled at a rate of 10 K.h⁻¹ down to 673 K, after which the furnace was turned off. The crystals obtained by washing the final product with warm water, in order to dissolve the flux, are essentially composed by green crystals of $\text{AgCr}_2(\text{PO}_4)(\text{P}_2\text{O}_7)$.

2.3. Structure determination

The structure was determined from single X-ray data, collected at room temperature by an Enraf-Nonius CAD4 [8] diffractometer using monochromated Mo-K α radiation ($\lambda = 0.7107 \text{ \AA}$) and $\omega/2\theta$ scans. The unit cell parameters and the orientation matrix were determined from a least-squares fit of 25 reflections in the range $10.95^\circ \leq \theta \leq 14.98^\circ$. A total of 1401 unique reflections were measured ($R_{in} = 0.082$) but only 809 were considered as observed according to the statistic criterion [$I > 2\sigma(I)$].

The intensity data were corrected for Lorentz and polarization effects. Absorption corrections were done analytically taking into account the size and shape of the crystal ($T_{min} = (T_{min} = 0.20; T_{max} = 0.49)$). The structure was solved by direct methods [9], which allowed us to obtain the positions of the Cr and Ag atoms. The P and O atoms were subsequently localized by inspection of the difference electron density maps [10].

At this stage the atomic coordinates and isotropic thermal factors were refined to $R = 0.131$ and $R_w = 0.346$. When all the atoms were anisotropically refined, the agreement factors R and R_w converged to 0.050 and 0.159, respectively but the difference synthesis map shows strong electronic residues at 0.247, 0.187, and 0.518, which allowed us to think that the four silver atoms of the cell are spread randomly over eight positions. All these positions cannot be fully occupied at the same time because two position related by a symmetry center are distant by only 0.33 Å. Finally, when all the atoms were anisotropically refined, the agreement factors R and R_w converged to 0.043 and 0.136 and all ADPs are positive with normal standard deviations. The cationic distribution was confirmed by a Bond Valence Sums (B. V. S.) calculation using the Brown and Altermatt method [11]. Experimental conditions for intensity measurements, structure solution and refinement are reported in Table 1. Final atomic coordinates and

Table 1

Details of the data collection and structural refinement for $\text{AgCr}_2(\text{PO}_4)(\text{P}_2\text{O}_7)$.

Crystal data	
Chemical formula	$\text{AgCr}_2(\text{PO}_4)(\text{P}_2\text{O}_7)$
Crystal system	Monoclinic
Space group	$C2/c$
a (Å)	11.493 (1)
b (Å)	8.485 (1)
c (Å)	8.790 (1)
β (°)	114.56 (1)
Z	4
ρ_{cal} (g.cm ⁻³)	4.095
Data collection	
Crystal dimensions	0.1 × 0.07 × 0.07 mm
Diffractometer	CAD4 (Enraf-Nonius)
Radiation	λ (Mo K α) = 0.7107 Å
Monochromator	Graphite
μ (mm ⁻¹)	5.903
Scan type	$\omega/2\theta$
Scan speed	Variable
$2\theta_{max}$ (°)	59.9
Number of unique reflections; R_{int}	809; $R_{int} = 0.082$
Number of observed reflections [$I > 2\sigma(I)$]	633
$F(000)$	912
Structural refinement	
Intensity corrections	Lorentz-polarisation
Absorption correction	Analytical (0.20, 0.49)
(T_{min} , T_{max})	
Structure solution	Direct Methods
Reliability factors	$R_1 = 0.043$; $wR_2 = 0.135$; $S = 1.21$
Number of parameters	86
($\Delta\rho$) _{max, min} /e. Å ⁻³	1.63; -1.89

equivalent isotropic displacement parameters are listed in Table 2.

Further details of the crystal structure investigation can be obtained from the Fachinformationszentrum Karlsruhe, 76344 Eggenstein-Leopoldshafen, Germany, (fax: +49 7247 808 666; crysdta@fz.karlsruhe.de on quoting the depository number CSD 422998.

3. Results

3.1. Description of the structure

The new compound $\text{AgCr}_2(\text{PO}_4)(\text{P}_2\text{O}_7)$ is isostructural to $\text{AgV}_2(\text{PO}_4)(\text{P}_2\text{O}_7)$ [12]. Its framework is formed by $[\text{PO}_4]$

Table 2

Atomic coordinates and displacement parameters U_{eq} (Å²) for $\text{AgCr}_2(\text{PO}_4)(\text{P}_2\text{O}_7)$.

Atom	Wyckoff	x (σ)	y (σ)	z (σ)	U_{eq} (σ)
Ag	8f	0.2563 (4)	0.2343 (4)	0.5109 (4)	0.0230 (1)
Cr	8f	-0.1258 (2)	0.2382 (1)	0.4593 (2)	0.0044 (1)
P1	8f	0.3883 (2)	0.0636 (1)	0.2870 (3)	0.0043 (2)
P2	4e	0	0.0434 (1)	0.25	0.0052 (1)
O1	4e	0.5	-0.0170 (4)	0.25	0.0082 (2)
O2	8f	-0.3101 (4)	0.1597 (1)	0.3738 (2)	0.0057 (2)
O3	8f	0.4512 (1)	0.1736 (4)	0.4365 (4)	0.0088 (2)
O4	8f	0.3116 (2)	-0.0683 (1)	0.3142 (3)	0.0074 (2)
O5	8f	0.0999 (2)	0.1517 (4)	0.2258 (3)	0.0112 (2)
O6	8f	0.5737 (4)	0.4482 (4)	0.4077 (1)	0.0129 (4)

Table 3
Main interatomic distances (Å) et angles (°) for $\text{AgCr}_2(\text{PO}_4)(\text{P}_2\text{O}_7)$.

CrO₆			
Cr-O(6)	1.905 (5)	O(6)-Cr-O(5)	94.6 (2)
Cr-O(5)	1.917 (4)	O(6)-Cr-O(3)	91.7 (2)
Cr-O(3)	1.971 (5)	O(5)-Cr-O(3)	93.1 (2)
Cr-O(4)	2.016 (3)	O(6)-Cr-O(4)	177.60 (19)
Cr-O(2)	2.044 (5)	O(5)-Cr-O(4)	85.1 (2)
Cr-O(2)	2.082 (4)	O(3)-Cr-O(4)	90.66 (19)
<Cr-O>	1.989 (4)	O(6)-Cr-O(2)	88.1 (2)
		O(5)-Cr-O(2)	93.7 (2)
		O(3)-Cr-O(2)	173.20 (18)
		O(4)-Cr-O(2)	89.52 (19)
		O(6)-Cr-O(2)	91.72 (19)
		O(5)-Cr-O(2)	168.7 (2)
		O(3)-Cr-O(2)	96.05 (19)
		O(4)-Cr-O(2)	88.18 (19)
		O(2)-Cr-O(2)	77.2 (2)
P(1)O₄			
P(1)-O(4)	1.506 (5)	O(4)-P(1)-O(3)	114.6 (3)
P(1)-O(3)	1.529 (5)	O(4)-P(1)-O(2)	112.4 (3)
P(1)-O(2)	1.555 (5)	O(3)-P(1)-O(2)	110.6 (3)
P(1)-O(1)	1.602 (6)	O(4)-P(1)-O(1)	106.6 (3)
<P(1)-O>	1.547 (5)	O(3)-P(1)-O(1)	107.6 (2)
P(2)O₄			
P(2)-O(6)	1.526 (5)	O(6)-P(2)-O(6)	116.0(4)
P(2)-O(6)	1.526 (5)	O(6)-P(2)-O(5)	110.5 (2)
P(2)-O(5)	1.556 (5)	O(6)-P(2)-O(5)	106.1 (3)
P(2)-O(5)	1.556 (5)	O(6)-P(2)-O(5)	106.1 (3)
<P(2)-O>	1.541 (5)	O(6)-P(2)-O(5)	110.5 (2)
		O(5)-P(2)-O(5)	107.4 (4)
AgO₇			
Ag-O(5)	2.429 (21)	Ag-O(5)	2.473 (22)
Ag-O(4)	3.086 (19)	Ag-O(6)	3.098 (20)
Ag-O(3)	2.614 (26)	Ag-O(4)	2.857 (19)
		Ag-O(3)	2.727 (20)
		<Ag-O>	2.755 (20)

tetrahedra, $[\text{P}_2\text{O}_7]$ groups and $[\text{CrO}_6]$ octahedral. Projection of the structure along ac plan is depicted in Fig. 1.

The projection of the structure along ab plan (Fig. 2) shows that it can be described as the stacking along b of octahedral layers and tetrahedral layers alternatively.

The structure can be described as the stacking along c direction of $[\text{Cr}_2\text{P}_3\text{O}_{16}]_\infty$ layers parallel to (001) two successive layers being enantiomorphic with respect to each other. As it is shown in Fig. 3, each layer consists of $[\text{Cr}_2\text{P}_2\text{O}_{14}]_\infty$ chains running along $[110]$ direction and built

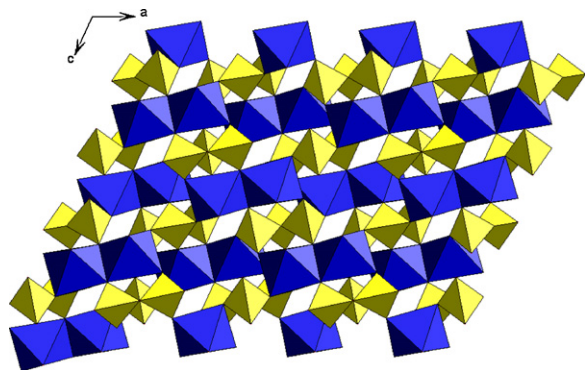


Fig. 1. A projection along the ac plan of $\text{AgCr}_2(\text{PO}_4)(\text{P}_2\text{O}_7)$.

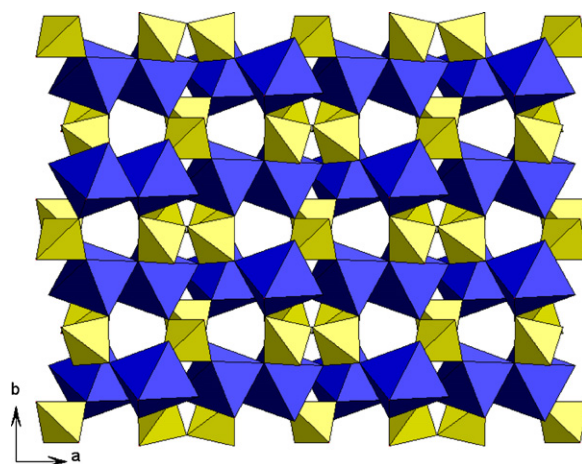


Fig. 2. A projection along the ab plan of $\text{AgCr}_2(\text{PO}_4)(\text{P}_2\text{O}_7)$.

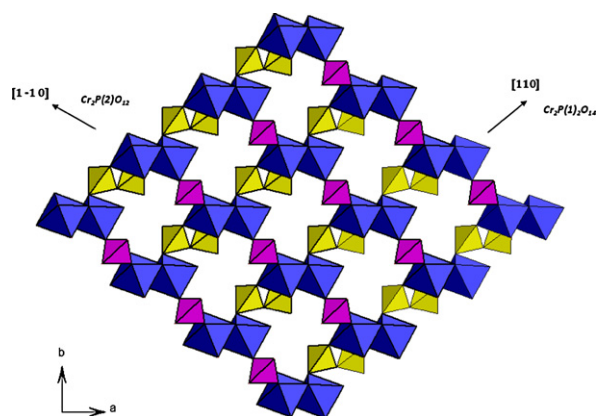


Fig. 3. Connection between the CrO_6 octahedron and its neighboring PO_4 tetrahedra.

up from Cr_2O_{10} bioctahedral units sharing their corners with diphosphate P_2O_7 groups laterally. These chains are interconnected through the monophosphate groups.

Another way to describe this structure is to consider the $[\text{Cr}_2\text{PO}_{12}]_\infty$ chains built up of corner sharing Cr_2O_{10} and monophosphate groups running along $[1-10]$ direction. These chains are interconnected through $[\text{P}_2\text{O}_7]$ groups.

A projection along the $[111]$ direction of $\text{AgCr}_2(\text{PO}_4)(\text{P}_2\text{O}_7)$ shows the six-edged tunnels occupied by the Ag^+ ions (Fig. 4).

In what follows, we will describe the structural environment for each atom.

3.1.1. Chromium atoms

The CrO_6 octahedron is rather irregular; with the smallest and largest distances being in the range from 1.905 (5) Å to 2.082 (4) Å. Average Cr–O distances is 1.989 (5) Å. This value is close to the ionic radii sum (2.02 Å) of Cr^{3+} and O^{2-} [13]. Each $[\text{CrO}_6]$ octahedron shares one common edge (O(2)–O(2)) with itself to forms $[\text{Cr}_2\text{O}_{10}]$ dimers with a Cr–Cr distance of 3.225 (6) Å and all of its corners with six $\text{P}(1)_2\text{O}_7$ and four $\text{P}(2)\text{O}_4$.

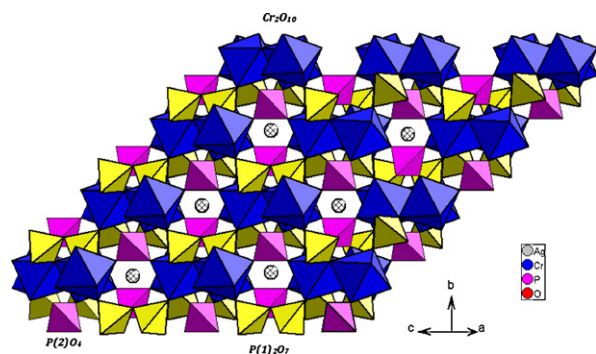


Fig. 4. A projection along the [111] direction of $\text{AgCr}_2(\text{PO}_4)(\text{P}_2\text{O}_7)$ showing the six-edged tunnels, occupied by the Ag^+ ions.

The O–Cr–O bond angle ranging from $77.2(2)^\circ$ to $96.05(2)^\circ$ and from $168.70(2)^\circ$ to $177.60(2)^\circ$ for the *cis* and *trans* angles, respectively (Table 3).

3.1.2. Phosphorus atoms

The particularity in these phosphates is the fact that $[\text{PO}_4]$ and $[\text{P}_2\text{O}_7]$ groups coexist in the same compound. The $[\text{PO}_4]$ tetrahedral are slightly distorted due to the corner sharing with $[\text{CrO}_6]$ polyhedra.

The diphosphate unit $\text{P}(1)_2\text{O}_7$ also adopts a binary internal symmetry with the bridging oxygen O(1) located into a two-fold axis. The average values for the P–O distances and P–O–P angles are $1.547(5) \text{ \AA}$, $109.45(2)^\circ$ respectively for $[\text{P}(1)\text{O}_4]$ tetrahedra. All these distances and angles are of the same magnitude in accordance with previous observations of $[\text{PO}_4]$ tetrahedra involved in other diphosphate anions [14–16]. This group shares the terminal oxygen atoms with four $[\text{Cr}_2\text{O}_{10}]$ dimers.

The $\text{P}(2)\text{O}_4$ tetrahedron is bonded to four different $[\text{CrO}_6]$ octahedral. The $\text{P}(2)$ –O distances range from $1.526(3) \text{ \AA}$ to $1.557(5) \text{ \AA}$ (av. 1.541 \AA) and the O–P–O angles are in the 106.1° – 116.0° range (av. 109.43°), which is in a good agreement with those previously observed. The calculated average values of the distortion indices [17], corresponding to the different angles and distances in both $[\text{P}(2)\text{O}_4]$ and $[\text{P}(1)\text{O}_4]$ tetrahedra $DI(\text{O}–\text{P}–\text{O}) = 0.25$ – 0.028 ; $DI(\text{P}–\text{O}) = 0.009$ – 0.019 and $DI(\text{O}–\text{O}) = 0.016$ – 0.021] exhibit a pronounced distortion of the $\text{P}(1)$ –O distances and O– $\text{P}(1)$ –O angles; so each phosphate group can be considered as a rigid regular arrangement of oxygen atoms (Table 4).

If we consider only Ag–O distances less than 3.1 \AA , the Ag cations are surrounded by seven oxygen atoms, with distances ranging from $2.429(21) \text{ \AA}$ to $3.098(20) \text{ \AA}$ forming

Table 4
ID for the coordination polyhedra around Cr and P.

	Cr	P1	P2
ID_d	0.029	0.019	0.009
ID_a	0.044	0.028	0.025
ID_o	0.037	0.021	0.016

$ID_d = \sum_{i=1}^{n1} \frac{|d_i - dm|}{n1 \cdot dm}$, $ID_a = \sum_{i=1}^{n2} \frac{|a_i - am|}{n2 \cdot am}$, $ID_o = \sum_{i=1}^{n2} \frac{|O_i - Om|}{n2 \cdot Om}$, d, a, o signify Cr/P–O bond distance, O–Cr/P–O angle and O–O edge within the relevant polyhedron; index *i* indicates individual values, index *m* the mean value for the polyhedron. *n1* and *n2* are 4 and 6 for the phosphate tetrahedra and 6 and 12 for the chrome octahedral.

irregular coordination polyhedra. The bond valence sum [18] calculations confirm the one, three and five-fold valence of the Ag, Cr and P atoms, respectively.

3.2. IR spectroscopic investigation

3.2.1. PO_4^{3-} vibrations

The internal vibrational modes of a free PO_4^{3-} tetrahedron with T_d symmetry are decomposed as $A_1 + E + 2T_2$. The mode with the A_1 symmetry type is the symmetric stretching mode (ν_1) of the P–O bonds. The modes with the E and T_2 symmetry types are bending O–P–O modes (ν_2 and ν_4 , respectively). The second mode with the T_2 symmetry is the asymmetric stretching mode (ν_3). For a free PO_4^{3-} tetrahedron, $\nu_1 = 938 \text{ cm}^{-1}$, $\nu_2 = 420 \text{ cm}^{-1}$, $\nu_3 = 1017 \text{ cm}^{-1}$ and $\nu_4 = 567 \text{ cm}^{-1}$.

3.2.2. $\text{P}_2\text{O}_7^{4-}$ vibrations

According to Corbridge [19], the P_2O_7 group (which can be written $\text{O}_3\text{P}–\text{O}–\text{PO}_3$) can be described for the vibration spectrum interpretation as an assembly of the vibrations of the PO_3 , and the P–O–P groups. The assignment of the $\text{P}_2\text{O}_7^{4-}$ modes is carried out in terms of PO_3 and P–O–P vibrations. In these conditions, the infrared bands for $\text{AgCr}_2(\text{PO}_4)(\text{P}_2\text{O}_7)$ shown in Fig. 5 are distributed in four distinct wave number ranges, 400 – 675 cm^{-1} , 720 – 800 cm^{-1} , 850 – 990 cm^{-1} , and 990 – 1400 cm^{-1} . Band assignments for the fundamental modes of this compound are given in Table 5 confirm the presence of the mono and diphosphate groups in the title compound.

3.3. Ionic conductivity

Typical complex plots of imaginary part of impedance– Z'' versus the real part Z' at various temperatures ($Z^* = Z' - jZ''$) are shown in Fig. 6 in which semi circles are observed. The centers of these semicircles are depressed below the baseline. The ionic conductivity as function of the temperature has been obtained from the values of intercept of the extrapolated high-frequency semicircles with the real axis. It should be noticed that conductivity in this phosphate is of ionic type; the electronic conductivity in oxides is due to overlapping of non-completely filled d

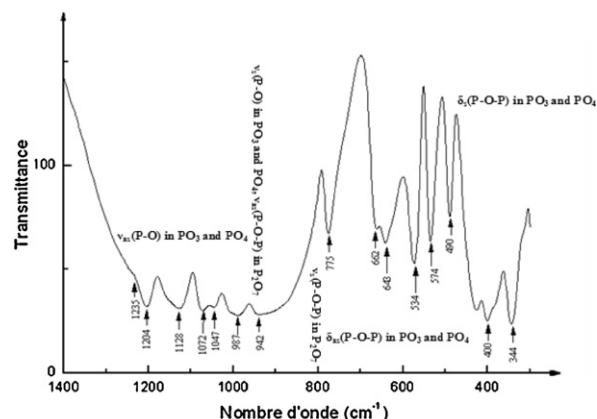


Fig. 5. Infrared analysis spectrum of $\text{AgCr}_2(\text{PO}_4)(\text{P}_2\text{O}_7)$.

Table 5
Band assignment (cm^{-1}) for $\text{AgCr}_2(\text{PO}_4)(\text{P}_2\text{O}_7)$.

Bands (cm^{-1})	Assignment
1235, 1204, 1128, 1072, 1047	$\nu_{\text{as}}(\text{P-O})$ in PO_3 and PO_4
987, 942	$\nu_{\text{s}}(\text{P-O})$ in PO_3 and PO_4 , $\nu_{\text{as}}(\text{P-O-P})$ in P_2O_7
775	$\nu_{\text{s}}(\text{P-O-P})$ in P_2O_7
662, 643, 575, 534	$\delta_{\text{as}}(\text{P-O-P})$ in PO_3 and PO_4
490, 425, 400	$\delta_{\text{s}}(\text{P-O-P})$ in PO_3 and PO_4

or f orbitals of cations or to electron hopping from aliovalent ions, assisted by an oxygen anion. In this case, we would exclude both mechanisms so conductivity should be totally ionic, some electronic could be present in grain boundaries, but negligible.

The conductivity variation indicates an increase of conductivity with rise in temperature with a typical Arrhenius-type behavior having linear dependence of thermal conductivity logarithm $\log(\sigma T)$ on inverse of temperature $10^3/T$ (K^{-1}) (Fig. 7). This type of temperature dependence of the conductivity indicates that the electrical conduction in the material is a thermally activated process. It can be explained in accordance with the

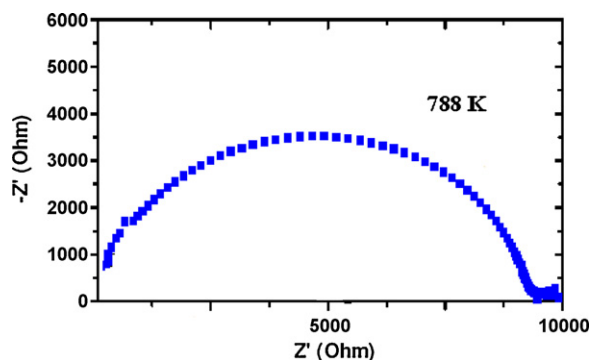


Fig. 6. Complex impedance diagram for $\text{AgCr}_2(\text{PO}_4)(\text{P}_2\text{O}_7)$ at 788 K.

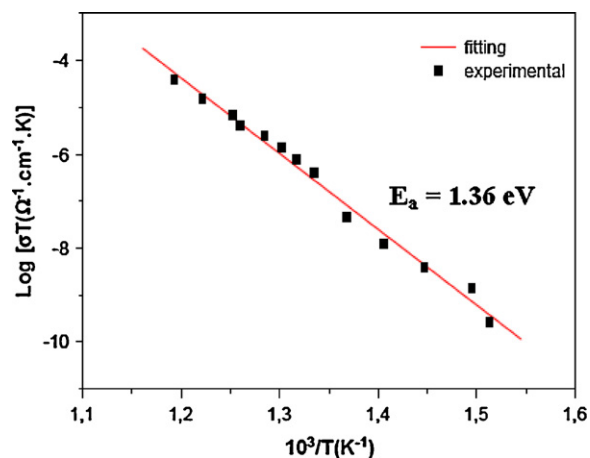


Fig. 7. Arrhenius plots of conductivity for $\text{AgCr}_2(\text{PO}_4)(\text{P}_2\text{O}_7)$ single crystals.

Table 6
Ionic conductivity (σ) of $\text{AgCr}_2(\text{PO}_4)(\text{P}_2\text{O}_7)$.

T(K)	R(Ω)	$\sigma(\Omega^{-1}\text{cm}^{-1}) \cdot 10^7$
661	588,848	1.04
669	238,416	2.15
691	193,451	3.16
711	118,222	5.17
731	68,600	8.9
749	27,311	22.36
759	20,994	29.08
768	16,223	37.64
778	12,759	47.86
788	10,480	58.27
798	8,427	72.45
818	6,210	98.33
838	4,253	143.58

expression: $\sigma T = A_0 \exp(-E_a/kT)$, where A_0 is the pre-exponential factor, E_a the activation energy, T the absolute temperature and k the Boltzmann constant. The conductivity value is $\sigma = 58.27 \times 10^{-7} \Omega^{-1} \text{cm}^{-1}$ at 788 K (Table 6) and the ionic jump activation energy is 1.36 eV. This material shows low conductivity performances, as compared to other compounds [20–24], this probably can be explained by other unfavorable structure features: ions Ag^+ lie in too small polyhedral as mentioned in the discussion above and are lying with completely occupation site.

4. Conclusions

Crystal structure of $\text{AgCr}_2(\text{PO}_4)(\text{P}_2\text{O}_7)$ has been resolved in C2/c space group. The structure was solved by direct methods. It was refined to $R = 0.043$ ($R_w = 0.135$) for 809 independent reflexions. Two kinds of $[\text{PO}_4]$ exist and the mean value of P–O is 1.547 (5) Å for one and 1.541 (5) Å for the other. In P_2O_7 , the angle P–O–P is 129.4 (5)°. The distances P–O of bridge are 1.602(4) Å, the mean value of P–O in terminals PO_3 is 1.530 Å. The structure contains tunnels along the [101] directions in which the Ag^+ ions are located. The coordination numbers of the silver ions are ten. The open framework of the title compound and the location of the silver ions in its tunnels make it a possible candidate for ionic conductivity. However, this material shows low conductivity performances with a conductivity value of $\sigma = 58.27 \times 10^{-7} \Omega^{-1} \text{cm}^{-1}$. The compound was also characterized by infrared spectroscopy and the results are in a good agreement with structural data.

Acknowledgements

I thank Dr. Amor Haddad (Laboratoire de matériaux et cristallographie [LMC], institut supérieure des sciences appliquées et technologie, avenue El Mourouj, 5111 Mahdia, Tunisia).

References

- [1] M. Pintard-Scrépel, F. d'Yvoire, F. Rémy, C.R. Acad. Sci. Paris Ser. C 286 (1978) 381.
- [2] F. d'Yvoire, M. Pintard-Scrépel, E. Bertey, M. de la Rochère, Solid State Ionics 851 (1983) 9.

- [3] C. Delmas, J.-C. Viala, R. Olazcuaga, G. le Flem, P. Hagenmuller, *Solid State Ionics* 209 (1981) 3.
- [4] I.S. Iyubutin, O.K. Melnikov, S.E. Sigaryov, V.G. Tersiev, *Solid State Ionics* 31 (1988) 197.
- [5] M. De la Roche're, A. Kahn, F. D'Yvoire, E. Bretey, *Mater. Res. Bull.* 20 (1985) 27.
- [6] C. Masquelier, F. d'Yvoire, N. Rodier, J. *Solid State Chem.* 95 (1991) 156.
- [7] C. Masquelier, F. d'Yvoire, E. Bertey, P. Berthet, C. Peytour-chansac, *Solid State Ionics* 67 (1994) 183.
- [8] CAD-4 Express Software. Enraf-Nonius Delft the Netherlands. 1994.
- [9] A. Altomare, G. Casciarano, C. Giacovazzo, A. Guagliardi, *J. Appl. Crystallogr.* 26 (1993) 43.
- [10] G.M. Sheldrick, SHELXL97, a program for the solution of the crystal structures, University of Göttingen, 1997.
- [11] I.D. Brown, D. Altermatt, *Acta Crystallogr.* B41 (1985) 244.
- [12] A. Grandin, A. Leclaire, B. Borel, J. Raveau, *Solid State Chem.* 115 (1995) 521.
- [13] R.D. Shannon, C.T. Prewitt, *Acta Cryst.* B25 (1969) 925.
- [14] M. Fakhfakh, S. Oyetola, N. Jouini, A. Verbaere, Y. Piffard, *Mater. Res. Bull.* 29 (1994) 97.
- [15] G.S. Gopalakrishna, B.H. Doreswamy, M.J. Mahesh, M. Mahendra, M.A. Sridhar, J.S. Prasad, K.G. Ashamanjari, *Bull. Mater. Sci.* 28 (1) (2005) 1.
- [16] J. Bennazha, F. Erragh, A. Boukhari, E.M. Holt, *J. Chem. Cryst.* 30 (2000) 705.
- [17] W.H. Baur, *Acta Cryst.* B30 (1974) 1195.
- [18] I.D. Brown, D. Altermatt, *Acta Cryst.* B41 (1985) 244.
- [19] D.E. Corbridge, in: M. Grayson, G. Wiley (Eds.), *Topics in Phosphorus Chemistry*, Griffith Ed, New York, 1966, 275 p.
- [20] J.M. Winand, *C. R. Acad. Sci. Paris, Ser II* (309) (1990) 1475.
- [21] S. Ledain, A. Leclaire, M.M. Borel, M. Hervieu, J. Provost, B. Raveau, *J. Solid State Chem.* 144 (1999) 297.
- [22] J.M. Winand, A. Rulmont, P. Tarte, *J. Solid State Chem.* 87 (1990) 83.
- [23] Y.F.Y. Yao, J.T. Kummer, *J. Inorg. Nucl. Chem.* 29 (1967) 2453.
- [24] J.B. Goodenough, H.Y.P. Hong, J.A. Kafalas, *Mater. Res. Bull.* 11 (1976) 203.